REGULAR ARTICLE

blood advances

Inhibition of ATR acutely sensitizes acute myeloid leukemia cells to nucleoside analogs that target ribonucleotide reductase

Sarah E. Fordham,[1] Helen J. Blair,[1] Claire J. Elstob,[1] Ruth Plummer,[1] Yvette Drew,[1] Nicola J. Curtin,[1] Olaf Heidenreich,[1] Deepali Pal,[1] David Jamieson,[1] Catherine Park,[1] John Pollard,[2] Scott Fields,[2] Paul Milne,[3] Graham H. Jackson,[4] Helen J. Marr,[4] Tobias Menne,[4] Gail L. Jones,[4] and James M. Allan[1]

[1]Newcastle Cancer Centre, Northern Institute for Cancer Research, Newcastle University, Newcastle upon Tyne, United Kingdom; [2]Vertex Pharmaceuticals (Europe) Ltd, Abingdon, Oxfordshire, United Kingdom; [3]Institute of Cellular Medicine, Newcastle University, Newcastle upon Tyne, United Kingdom; and [4]Department of Haematology, Freeman Hospital, Newcastle upon Tyne Hospitals National Health Service Foundation Trust, Newcastle upon Tyne, United Kingdom

Key Points

- Loss of ATR signaling is cytotoxic to AML cells in combination with gemcitabine and hydroxyurea via the induction of replication stress.
- A small molecule inhibitor of ATR in combination with gemcitabine completely eradicates AML in an orthotopic xenograft mouse model.

The ataxia telangiectasia and Rad3-related (ATR) protein kinase promotes cancer cell survival by signaling stalled replication forks generated by replication stress, a common feature of many cancers including acute myeloid leukemia (AML). Here we show that the antileukemic activity of the chemotherapeutic nucleoside analogs hydroxyurea and gemcitabine was significantly potentiated by ATR inhibition via a mechanism involving ribonucleotide reductase (RNR) abrogation and inhibition of replication fork progression. When administered in combination with gemcitabine, an inhibitor of the M1 RNR subunit, the ATR inhibitor VX-970, eradicated disseminated leukemia in an orthotopic mouse model, eliciting long-term survival and effective cure. These data identify a synergistic interaction between ATR inhibition and RNR loss that will inform the deployment of small molecule inhibitors for the treatment of AML and other hematologic malignancies.

Introduction

Oncogene expression drives cell proliferation and induces DNA replication stress via the dysregulation of pathways essential for replication origin firing and fork progression.[1] Replication stress promotes genomic instability and renders cancer cells overly reliant on DNA damage response (DDR) pathways to maintain proliferation and survival. Ataxia telangiectasia and Rad3-related (ATR) serine/threonine protein kinase phosphorylates CHK1 in response to stalled replication forks.[2-6] Activation of the ATR-CHK1 DDR pathway leads to cell cycle arrest and invokes mechanisms that prevent replication fork breakage and premature mitotic entry before replication is completed.[1]

Acute myeloid leukemia (AML) is a genetically heterogenous malignancy characterized by recurrent acquired somatic alterations that alter cell proliferation and differentiation leading to an accumulation of immature blast cells in the bone marrow. Although many AML patients achieve complete morphologic remission with nucleoside analog and anthracycline-based therapies, the 3-year survival is less than 30%.[7] Many of the somatic driver mutations in AML are associated with the induction of replication stress, including *MLL* (*KMT2A*) gene fusions and mutations in *TP53*, *RAS*, and *c-MYC*.[8,9] Efficient DDR signaling, mediated via ATR-CHK1 signaling, is implicated in maintaining leukemia cell survival.

The induction of replication stress is also a key feature of chemotherapy agents used to treat AML, including nucleoside analogs such as cytarabine, clofarabine, gemcitabine, and hydroxyurea,[10] which are efficacious via a mechanism in which DDR pathways become overwhelmed by high levels of DNA damage-induced replication stress. We hypothesized that targeted inhibition of ATR-CHK1 signaling combined with replication-stalling chemotherapy agents would generate a therapeutic window for treating AML with high levels of endogenous replication stress. Here, we show that co-treatment with an ATR inhibitor significantly

Submitted 13 December 2017; accepted 9 April 2018. DOI 10.1182/bloodadvances.2017015214.

The full-text version of this article contains a data supplement.

potentiates the antileukemic effects of hydroxyurea and gemcitabine in AML cell lines and primary AML samples and completely eradicates disseminated leukemia in an orthotopic mouse model of AML. We also show that ATR inhibition is particularly efficacious in combination with those chemotherapy agents that inhibit ribonucleotide reductase (RNR), including hydroxyurea and particularly gemcitabine.

Materials and methods

Cell lines

HL-60, AML-2, AML-3, U937, THP-1, NB4, and MV4-11 cell lines were from DSMZ (Braunschweig, Germany). MV4-11 pSLIEW cells are a subclone of MV4-11 engineered to express firefly luciferase. HL-60 ATRi (con) and HL-60 ATRi (ind) are subclones of HL-60 with knockdown of *ATR*. Cells were maintained in culture medium (CM) (RPMI 1640 medium supplemented with 10% fetal bovine serum [FBS] and 50 μg/mL penicillin/streptomycin) at 37°C in a humidified 5% CO_2 incubator.

HEK293T cells were maintained in *N*-2-hydroxyethylpiperazine-*N*′-2-ethanesulfonic acid–modified Dulbecco's modified Eagle medium 6171 supplemented with 10% FBS, 50 μg/mL penicillin/streptomycin, 4 mM L-glutamine, 1 mM sodium pyruvate, and 500 μg/mL G418. The identity of cell lines was confirmed by short tandem repeat profiling (NewGene, Newcastle upon Tyne, United Kingdom) and tested for mycoplasma using a MycoAlert kit (Lonza, Slough, United Kingdom).

Primary cultures

Diagnostic bone marrow aspirates were separated using Lymphoprep (Stemcell Technologies, Cambridge, United Kingdom). Patients included de novo AML1 (male, age 76 years), de novo AML2 (male, age 72 years), de novo AML3 (female, age 66 years), de novo AML 4 (female, age 52 years), relapsed AML (female, age 56 years), therapy-related AML1 (t-AML) (pediatric male, previous chemotherapy for acute lymphoblastic leukemia), and t-AML2 (male, previous chemotherapy for bowel cancer and chronic myeloid leukemia). Mononuclear cells were washed in phosphate-buffered saline and resuspended in enhanced CM (Iscove's modified Dulbecco's medium supplemented with 20% FBS, 4 mM L-glutamine, 50 μg/mL penicillin/streptomycin, 10 ng/mL interleukin-3, and 20 ng/mL stem cell factor) for use in cytotoxicity assays. Samples were collected after informed consent was provided via the Newcastle Haematology Biobank (Ref: 12/NE/0395).

Normal bone marrow cells were obtained from 2 females (age 50 and 57 years) undergoing surgery for osteoarthritis. Samples were collected after informed consent was provided and after approval by the Newcastle and North Tyneside 1 Research Ethics Committee (Ref: 09/H0906/72).

In vivo mouse studies

Female 8-week old *Rag2*$^{-/-}\gamma c^{-/-}$ mice (*Rag2*$^{-/-}$*Il2rg*$^{-/-}$129×Balb/c) were used for in vivo investigations[11] in accordance with United Kingdom Home Office Project License PPL60/4552. For intrafemoral injection, 5×10^5 MV4-11 Luc$^+$GFP$^+$ cells in 20 μL CM were injected through the knee into the femur marrow cavity. Mice underwent regular noninvasive whole body imaging starting 7 days postinjection. Anesthetized mice were injected intraperitoneally with 150 mg/kg luciferin and imaged using an IVIS Spectrum in vivo imaging system (Caliper Life Sciences, Waltham, MA). Total flux bioluminescence was quantitated in photons/second (p/s). Mice received either 100 mg/kg gemcitabine (days 1, 4, 8, and 12), 60 mg/kg VX-970 (days 1-5 and 8-12), both 100 mg/kg gemcitabine (days 1, 4, 8, and 12) and 60 mg/kg VX-970 (days 1-5 and 8-12), or vehicle only. Gemcitabine (20 mg/mL in saline) was administered intraperitoneally, and VX-970 (12 mg/mL in D-α-tocopherol polyethylene glycol 1000 succinate) was administered by oral gavage.

Mice were monitored for signs of disease progression and were humanely euthanized if tumor diameter reached 15 mm or before this point if there were any signs of animal suffering. Tissues harvested during postmortem analysis were fixed in 10% neutral buffered formalin, decalcified in 10% formic acid, and paraffin embedded and sectioned at 4 μm. Serial sections were stained for the human markers CD33, CD45, and Ki67 or with hematoxylin and eosin for morphologic assessment by the Department of Pathology, Royal Victoria Infirmary (Newcastle upon Tyne, United Kingdom).

Generation of cells with ATR knockdown

HL-60 ATRi (con) cells with constitutive ATR knockdown were generated with verified ATR MISSION short hairpin RNA (shRNA) lentiviral transduction particles (Sigma-Aldrich, Dorset, United Kingdom). Briefly, lentiviral particles were incubated with cells in CM supplemented with 8 μg/mL hexadimethrine bromide and centrifuged at 800*g* for 30 minutes at 32°C. HL-60 non-target control cells were generated using MISSION non-target shRNA control transduction particles. Transduced cells were selected for with 2 μg/mL puromycin.

For generation of HL-60 ATRi (ind) cells with inducible *ATR* knockdown, shRNA lentivirus was produced by transfection of HEK293T cells with the packaging vector pCMVΔ8.91, the envelope vector pMD2.G, and a TRIPZ inducible lentiviral human ATR shRNA (GE Healthcare, Buckinghamshire, United Kingdom). The expression of *ATR* shRNA was induced by supplementing CM with 500 ng/mL doxycycline 48 hours before setting up cytotoxicity assays.

Transient *RRM1* knockdown using siRNA

Exponentially growing cells were mixed with 1 μM Dharmacon siGENOME Human RRM1 (6240) small interfering RNA (siRNA) SMARTpool (GE Healthcare) or MISSION siRNA Universal Negative Control #1 (Sigma-Aldrich) and electroporated at 260 V for 10 ms.

Potentiation assays

Reagents used in potentiation assays were from Sigma-Aldrich unless otherwise stated. Gemcitabine, hydroxyurea, and clofarabine were reconstituted in sterile dH_2O. Cytarabine, fludarabine, 3-aminopyridine-2-carboxyaldehyde-thiosemicarbazone (3-AP), and the ATR inhibitors VE-821 (Axon Medchem, Groningen, The Netherlands) and VX-970 (Selleck Chemicals, Munich, Germany) were reconstituted in dimethyl sulfoxide (DMSO).

AML cell lines or primary mononuclear cells were seeded in CM or enhanced CM, respectively, supplemented with either ATR inhibitor or vehicle control. Cells were treated with increasing doses of cytotoxic agent (or control) and incubated for 96 hours. For AML cell lines, viable cells were identified by trypan blue dye exclusion and were counted using a hemocytometer. Then, 10 μg/mL resazurin sodium salt was added, plates were incubated for an additional 6 hours, and fluorescence was determined using a plate reader with excitation at 535 nm and emission at 590 nm. Survival fractions were determined at each drug concentration relative to vehicle controls. All assays were performed in triplicate and means ± standard deviation were calculated. Potentiation factors (PFs) were calculated as the fold difference in mean survival fraction between cells in the presence or absence of ATR inhibitor.

Combination index (CI) was calculated using Compusyn and the Chou-Talalay method[12] with quantitative definitions for additive effect (CI = 1), synergism (CI <1), and antagonism (CI >1) for VE-821 in combination with hydroxyurea or gemcitabine.

Patient-derived cells were cultured in cytokine-supplemented media, and proliferation was confirmed between 6 and 24 hours using the RealTime-Glo MT assay (Promega, Madison, WI) (supplemental Figure 1).

Cell cycle analysis

Exponentially growing cells were treated with 1 μM VE-821 (or DMSO control) and 10 nM gemcitabine, 100 μM hydroxyurea, or 100 nM cytarabine (or vehicle control). Aliquots were removed, and cells were fixed with ice-cold 70% (v/v) ethanol. Cells were resuspended in phosphate-buffered saline supplemented with 20 μg/mL RNase A and 40 μg/mL propidium iodide, incubated at room temperature in the dark for 10 minutes, and then analyzed using a BD FACSCalibur flow cytometer (BD Biosciences, San Jose, CA).

DNA fiber assay

MV4-11 cells were seeded in CM with 5 nM gemcitabine, 15 μM hydroxyurea, or 50 nM cytarabine for 1 hour and incubated with 25 μM 5-iodo-2′-deoxyuridine (IdU) for 40 minutes. Cells were resuspended in CM supplemented with drug as above, 250 μM 5-chloro-2′-deoxyuridine (CldU), and 1 μM VE-821 (or DMSO control) for an additional 40 minutes. Microscope slides were prepared as previously described,[13] and DNA fibers were studied by using a Leica DMR light microscope. IdU and CldU tract lengths were measured using ImageJ (Version 1.41o; National Institutes of Health) (conversion factor: 1 μm = 2.59 kb). A minimum of 100 forks were analyzed per treatment.

Western blotting

Cellular proteins were extracted using Phosphosafe (Millipore Ltd, Watford, United Kingdom) and quantified by using a Pierce bicinchoninic acid assay (Thermo Fisher Scientific, Cramlington, United Kingdom). Proteins were separated using Novex NUPAGE 3% to 8% tris-acetate gels (Invitrogen Life Technologies, Paisley, United Kingdom), transferred to nitrocellulose membranes, and immunoblotted. Antibodies were ATR (N-19; Santa Cruz Biotechnology, Heidelberg, Germany), pCHK1 (Ser345) (133D3; Cell Signaling Technology, Leiden, The Netherlands), RRM1 (A-10; Santa Cruz Biotechnology), glyceraldehyde-3-phosphate dehydrogenase (0411; Santa Cruz Biotechnology), and horseradish peroxidase–conjugated secondary antibodies (Agilent Technologies, Santa Clara, CA).

Statistical analysis

The Student *t* test (2-tailed), 2-way analysis of variance, or Mann-Whitney *U* test was used to compare responses in the presence and absence of ATRi. Overall survival data from mice were compared by Kaplan-Meier survival analysis using a Mantel-Cox log-rank test. All statistical tests were performed using GraphPad Prism 6 or IBM SPSS Statistics 22 software.

Results

Inhibition or RNA silencing of ATR potentiates hydroxyurea and gemcitabine in AML cell lines

Phosphorylation of checkpoint kinase CHK1 was used as a marker for ATR pathway activation. Treatment with 100 μM hydroxyurea resulted in phosphorylation of CHK1 in AML cell lines AML-2, AML-3, HL-60, MV4-11, NB4, THP-1, and U937 (Figure 1A). CHK1 phosphorylation was attenuated in all 7 AML cell lines when hydroxyurea was coadministered with the ATR inhibitor VE-821 (Figure 1A), demonstrating that the ATR signaling pathway is active in AML cells and that it can be inhibited by VE-821.

Treatment with VE-821 at a concentration (1 μM) that has no single-agent activity did not consistently potentiate the antiproliferative effects of cytarabine, clofarabine, or fludarabine (supplemental Figure 2), although there was some potentiation of clofarabine in MV4-11 and of fludarabine and cytarabine in THP-1 (supplemental Figure 2). However, there was consistent potentiation of hydroxyurea and particularly gemcitabine by VE-821 in all 7 AML cell lines tested (Figure 1B-C), and CI analysis confirmed that VE-821 is synergistic (CI <1) with hydroxyurea and gemcitabine (Figure 1D). AML cells were also treated with a second structurally unrelated ATR inhibitor (NU6027),[14] which also consistently potentiated the antiproliferative effects of hydroxyurea and gemcitabine (Figure 1B-C; supplemental Figure 2).

HL-60 cell clones expressing a constitutively active shRNA construct (HL-60 ATR [con]) or a doxycycline-inducible shRNA construct targeting ATR (HL-60 ATR [ind]) had reduced ATR protein expression compared with control-transduced cells (Figure 1E) and were sensitized to the antiproliferative effects of hydroxyurea and particularly gemcitabine (Figure 1F-G). In contrast, loss of ATR expression had weak or no effect on sensitivity to the antiproliferative effects of cytarabine, clofarabine, or fludarabine (supplemental Figure 3). These data demonstrate that loss of ATR function mediated by small molecule inhibition or RNA silencing sensitizes AML cells to the inhibitory effects of hydroxyurea and gemcitabine.

ATRi attenuates replication fork progression and induces S-phase arrest in combination with gemcitabine and hydroxyurea

ATR protects cells against collapsed replication forks under conditions of replicative stress.[4,5,15] We hypothesized that ATRi in combination with hydroxyurea or gemcitabine would lead to reduced replication fork progression and S-phase arrest. Treatment with ATR inhibitor alone did not affect the U937 cell cycle profile (Figure 2A), but single-agent gemcitabine induced S-phase arrest discernible between 8 and 16 hours that was resolved by 24 hours (Figure 2A). VE-821 potentiated gemcitabine-induced S-phase arrest (Figure 2A). This effect was also seen in cells after treatment with an approximate equitoxic concentration of hydroxyurea but was less pronounced (Figure 2A). Furthermore, treatment with 1 μM VE-821 significantly slowed replication fork progression in combination with hydroxyurea (PF, 1.37; $P < .001$) and particularly with gemcitabine (PF, 1.57; $P < .001$) (Figure 2B; supplemental Figure 4), consistent with the cell cycle results. Treatment of U937 cells with cytarabine also induced a pronounced S-phase arrest (Figure 2A) and replication fork arrest (supplemental Figure 4). However, co-treatment with 1 μM VE-821 did not potentiate either S-phase arrest or replication fork arrest (PF, 1.04; $P = .222$) (Figure 2A-B).

ATRi potentiates growth inhibition resulting from ribonucleotide reductase (RNR) knockdown

The anticancer activities of gemcitabine and hydroxyurea are partly mediated via inhibition of RNR, a protein involved in the de novo

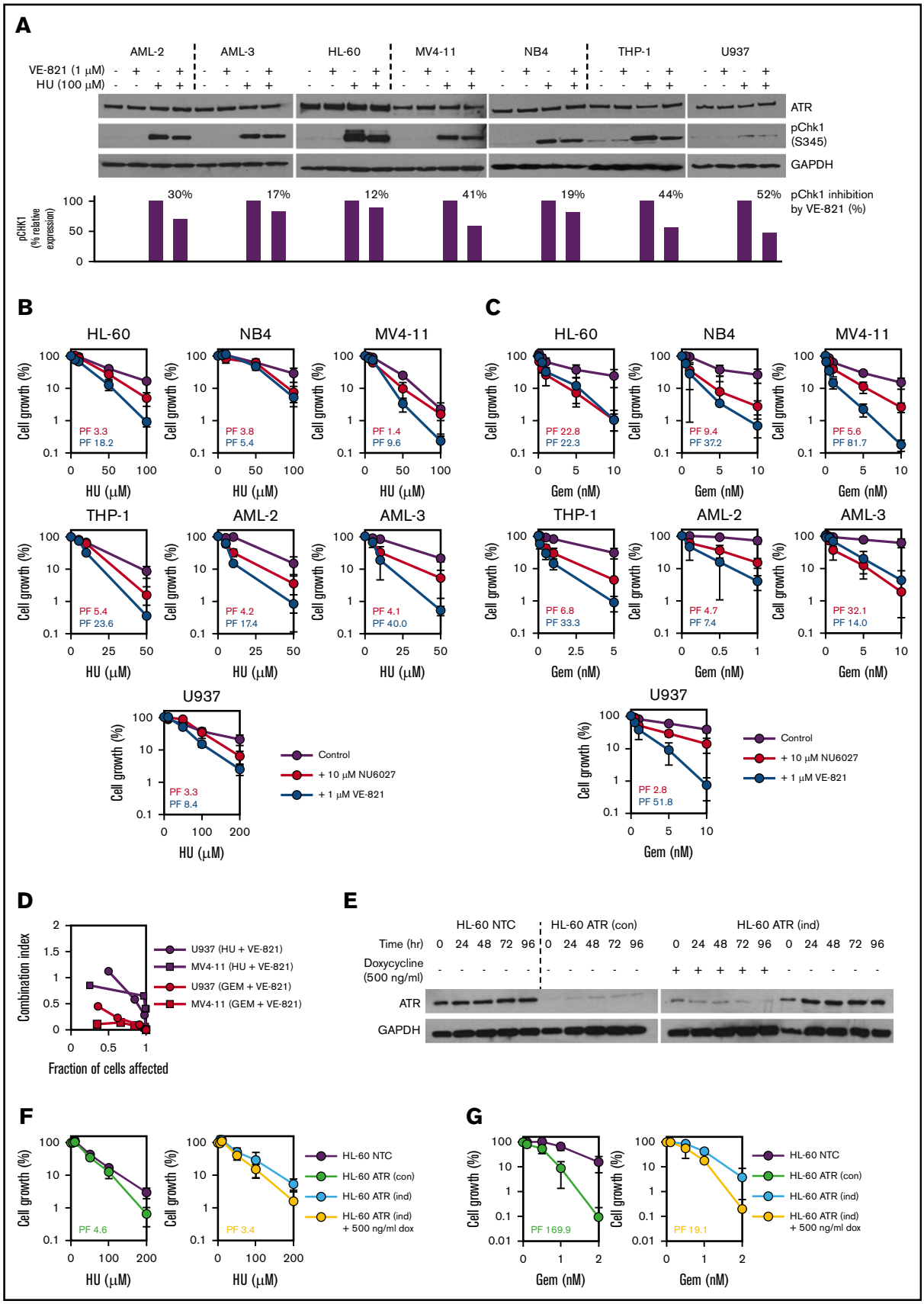
A
AML-2
AML-3
HL-60
MV4-11
NB4
THP-1
U937
VE-821 (1 μM)
HU (100 μM)
ATR
pChk1 (S345)
GAPDH
30%
17%
12%
41%
19%
44%
52%
pChk1 inhibition by VE-821 (%)
pCHK1 (% relative expression)
B
C
HL-60
NB4
MV4-11
THP-1
AML-2
AML-3
U937
Cell growth (%)
HU (μM)
Gem (nM)
PF 3.3
PF 18.2
PF 3.8
PF 5.4
PF 1.4
PF 9.6
PF 22.8
PF 22.3
PF 9.4
PF 37.2
PF 5.6
PF 81.7
PF 5.4
PF 23.6
PF 4.2
PF 17.4
PF 4.1
PF 40.0
PF 6.8
PF 33.3
PF 4.7
PF 7.4
PF 32.1
PF 14.0
PF 3.3
PF 8.4
PF 2.8
PF 51.8
Control
+ 10 μM NU6027
+ 1 μM VE-821
D
Combination index
Fraction of cells affected
U937 (HU + VE-821)
MV4-11 (HU + VE-821)
U937 (GEM + VE-821)
MV4-11 (GEM + VE-821)
E
HL-60 NTC
HL-60 ATR (con)
HL-60 ATR (ind)
Time (hr)
Doxycycline (500 ng/ml)
ATR
GAPDH
F
G
HL-60 NTC
HL-60 ATR (con)
HL-60 ATR (ind)
HL-60 ATR (ind) + 500 ng/ml dox
PF 4.6
PF 3.4
PF 169.9
PF 19.1

Figure 1.

biosynthesis of nucleotide precursors for DNA replication.[16] Reduced deoxyribonucleotide triphosphate (dNTP) levels after exposure to gemcitabine or hydroxyurea slows DNA replication fork progression and induces S-phase arrest.[17,18] Cellular response to the resulting stalled replication forks is mediated by ATR signaling.[19] Given this shared mechanism of action, we hypothesized that replication stalling as a result of loss of RNR expression is potentiated by ATRi.

Mammalian RNRs consist of 2 homodimeric subunits that associate to form a heterodimeric tetramer, with the larger RRM1 dimer containing the catalytic site and the smaller dimer consisting of 1 of 2 possible isoforms (RRM2 or RRM2B).[20] Treatment with gemcitabine induces cellular expression of RNR in pancreatic cancer cells,[21] possibly as a mechanism to compensate for inhibition of activity. Consistent with this model, we observed increased expression of RRM1 in AML-3 cells treated with gemcitabine and hydroxyurea but not with cytarabine (Figure 3A). Cotreatment with VE-821 inhibited drug-induced RRM1 upregulation, which was particularly apparent in gemcitabine-treated cells (Figure 3A), providing further evidence that the efficacy of this particular combination is mediated via abrogation of RNR. Consistent with this hypothesis, siRNA-mediated knockdown of RRM1 in AML-3 and U937 cells resulted in a robust pCHK1 response, which was attenuated by VE-821 (Figure 3B). Furthermore, growth inhibition mediated via RRM1 knockdown was also potentiated by VE-821 (Figure 3A). Treatment of cells with 3-AP, a non-nucleoside RNR inhibitor, induced a pCHK1 response in AML-2, AML-3, and U937 that was attenuated by VE-821 (Figure 3C). 3-AP exposure also reduced proliferation that was potentiated by ATRi in all 3 cell lines (Figure 3D). These data demonstrate that loss of RNR induces a pCHK1 response that is signaled via ATR and that attenuation of this pathway by VE-821 significantly potentiates the growth-inhibitory effects of RNR inhibition in AML cells.

ATRi potentiates the cytotoxicity of hydroxyurea and gemcitabine in primary AML samples ex vivo

The growth inhibitory effects of hydroxyurea and gemcitabine were potentiated by VE-821 in the majority of AML patient samples tested (Figure 4A-B), which included 3 adult patients with de novo AML, a relapsed AML, a pediatric t-AML patient (t-AML1), and an adult t-AML patient (t-AML2). Those samples in which potentiation was not observed seemed to be intrinsically chemotherapy resistant to either hydroxyurea (de novo AML3) or gemcitabine (t-AML2). In contrast to primary AML samples, ATRi did not potentiate the growth-inhibitory effects of hydroxyurea or gemcitabine in primary bone marrow cells from healthy donors (Figure 4C-D).

ATRi potentiates the cytotoxicity of gemcitabine in an orthotopic mouse model of AML

We next determined whether ATRi could potentiate the activity of gemcitabine in an orthotopic mouse model of AML treated with VX-970 (VE-822), an orally bioavailable derivative of VE-821.[22] We first confirmed that VX-970 mirrored results with VE-821 and demonstrated potentiation of hydroxyurea and gemcitabine in MV4-11 and primary AML cells (supplemental Figure 5A-B).

MV4-11 cells engineered to express firefly luciferase were intrafemorally transplanted into immunocompromised *Rag2*$^{-/-}$*gc*$^{-/-}$ mice. Bioluminescent imaging demonstrated localized femoral engraftment 7 days after injection, with signal developing in other parts of the body (liver, cranium, noninjected femur) between days 15 and 18 in untreated mice. Treatment was initiated 7 days after injection when disease was localized to the injected femur and before the emergence of luciferase signal elsewhere. Mice were treated with 100 mg/kg gemcitabine on days 1, 4, 8, and 11 and/or VX-970 on days 1-5 and 8-12. Treatment with gemcitabine monotherapy led to significant early disease control by the end of the 2-week treatment period (Figure 5A-B) and significantly improved overall survival compared with controls ($P = .001$; Figure 5C). Nevertheless, signal returned in all mice, and relapsed AML required the humane euthanasia of all animals randomly assigned to this arm. VX-970 monotherapy had no discernible effect on early disease control but did have a very modest effect on overall survival (Figure 5A-C). Treatment with gemcitabine and VX-970 combined conferred very significant early disease control, eliciting substantial reductions in signal by day 14 in all 6 mice randomly assigned to this arm (Figure 5A-B) and also conferred a significantly improved overall survival ($P = .001$; Figure 5C). Of the 6 animals in this arm, 1 was censored because of an unrelated condition on day 32 with no evidence of disease, 1 reached the specified humane end point (as a result of AML symptoms) on day 102, and 4 animals remained disease free when the experiment was terminated on day 165.

We next investigated the efficacy of gemcitabine plus VX-970 when treatment was delayed such that the luciferase signal was no longer localized to the femur but was disseminated to other parts of the body. As seen with localized disease, there was significant treatment-induced control of disseminated disease

Figure 1. ATR inhibition using small molecule inhibitors or shRNA-mediated gene knockdown potentiates the inhibitory effects of hydroxyurea (HU) and gemcitabine (Gem) in AML cell lines. (A) To confirm target engagement, AML cell lines were exposed to 100 μM HU (or vehicle control) for 1 hour in the presence of 1 μM VE-821 (or DMSO control), and western blotting was performed for ATR and pCHK1 (Ser345). Expression of pCHK1 is expressed relative to the HU-only lane for each cell line. (B-C) AML cell lines were treated with (B) HU or (C) Gem either alone (purple circles), in combination with 10 μM NU6027 (red circles), or in combination with 1 μM VE-821 (blue circles), and cell density (relative to respective vehicle controls) was determined after 96 hours. PFs were calculated for both ATR inhibitors (NU6027, red text; VE-821, blue text) at the highest dose of HU or Gem. (D) U937 and MV4-11 AML cells were treated with escalating does of VE-821 and/or drug (Gem or HU). CI values <1 indicate synergy between drug combinations. (E) Western blotting for ATR was performed at 24-hour intervals to confirm shRNA-mediated knockdown in HL-60 ATR (con) cells with constitutive ATR knockdown (left blot) and HL-60 ATR (ind) cells with doxycycline-induced ATR knockdown (right blot). (F-G) HL-60 ATR (con) cells (green circles, left chart) and HL-60 ATR (ind) cells (yellow circles, right chart) and their respective controls were treated with (F) HU or (G) Gem, and cell growth and PFs were determined as above. For all western blots, glyceraldehyde-3-phosphate dehydrogenase (GAPDH) was used as a loading control, and for all potentiation assays, data represent the mean ± standard deviation (SD) of 3 independent experiments. See supplemental Figures 2, 3, and 5A. dox, doxycycline; NTC, non-target control.

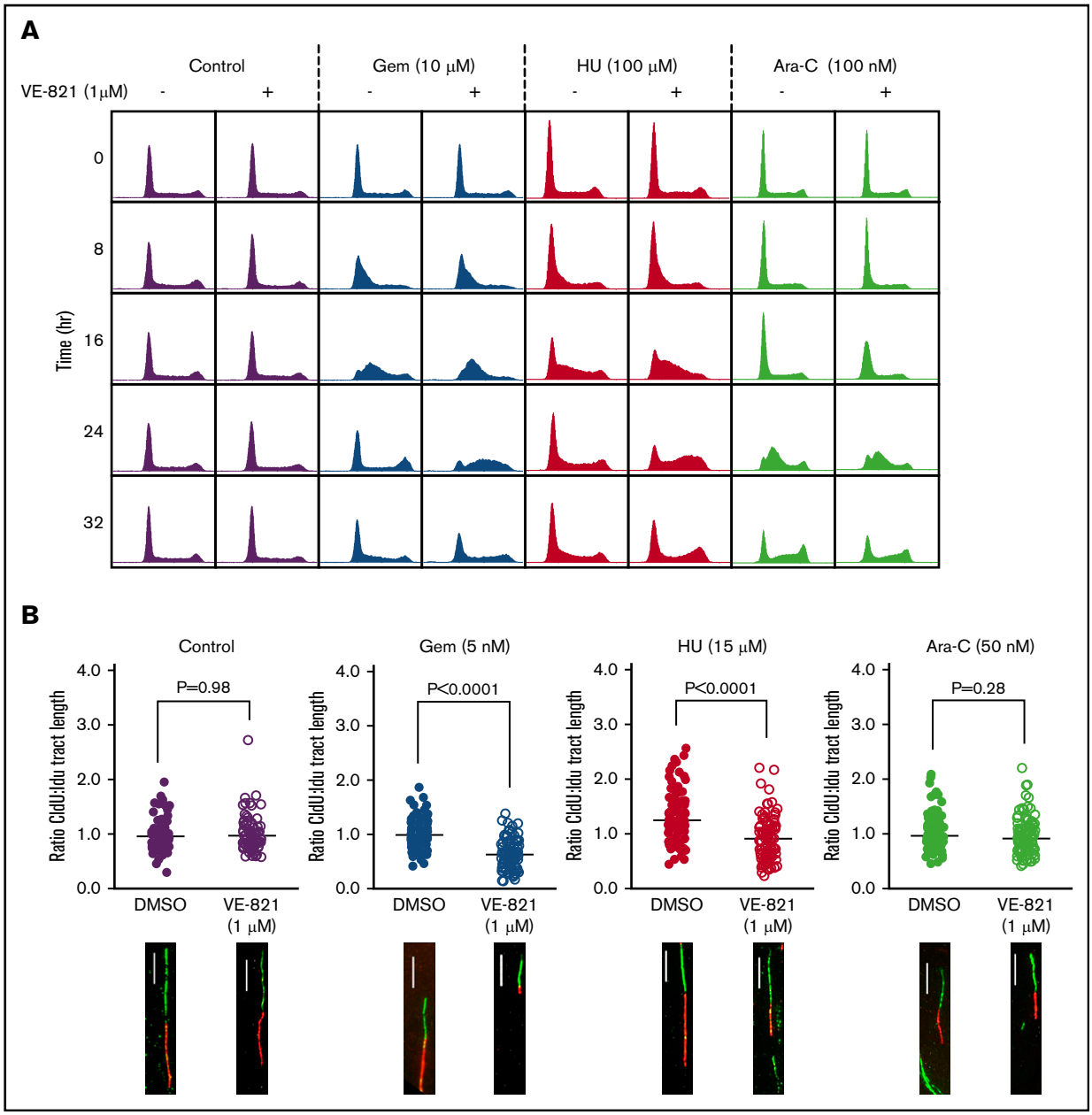

Figure 2. VE-821–mediated ATR inhibition attenuates cell cycle transit and replication fork progression in combination with HU and Gem (but not cytarabine [Ara-C]) in AML cell lines. (A) Unsynchronized populations of U937 cells were treated with 10 nM Gem, 100 μM HU, or 100 nM Ara-C (or vehicle control) in the presence of 1 μM VE-821 or DMSO control. Cell cycle profiles were determined by propidium iodide staining (in 2×10^5 cells) immediately pretreatment (0 hours) and at 8-hour intervals posttreatment, as indicated. (B) MV4-11 cells were preincubated with 5 nM Gem, 15 μM HU, 50 nM Ara-C, or vehicle control for 1 hour, then pulse labeled with 25 mM 5-iodo-2′-deoxyuridine (IdU) for 40 minutes, followed by 250 mM 5-chloro-2′-deoxyuridine (CldU) for 40 minutes (with maintenance of exposure to drug throughout). Treatment with 1 μM VE-821 or DMSO control was applied simultaneously with CldU. Data points represent ratios of CldU:IdU length in individual replication tracts in the presence (open circles) or absence (solid circles) of VE-821 from 3 independent experiments. Solid lines indicate mean ratios. *P* values were calculated using the Mann-Whitney *U* test. Images below charts are representative images of individual replication tracts with IdU in green and CldU in red. Scale bars represent 10 μm. See supplemental Figure 4.

with complete eradication of luciferase signal in 4 of 6 mice 7 days after the end of the second treatment cycle (supplemental Figure 6). Of the 6 animals treated, 4 eventually reached specified humane end points resulting from AML (days 64, 71, 88, and 143), but 2 had no evidence of luciferase signal (or disease) when the experiment was terminated on day 143. Histologic examination of tissues from these mice confirmed the absence of human AML markers at the termination of the experiment (Figure 6A). There was no evidence of bone marrow dysmorpology in nonengrafted animals treated with single-agent VX-970, which provides further evidence supporting the safe use of ATR inhibitors as therapy in AML (Figure 6B).

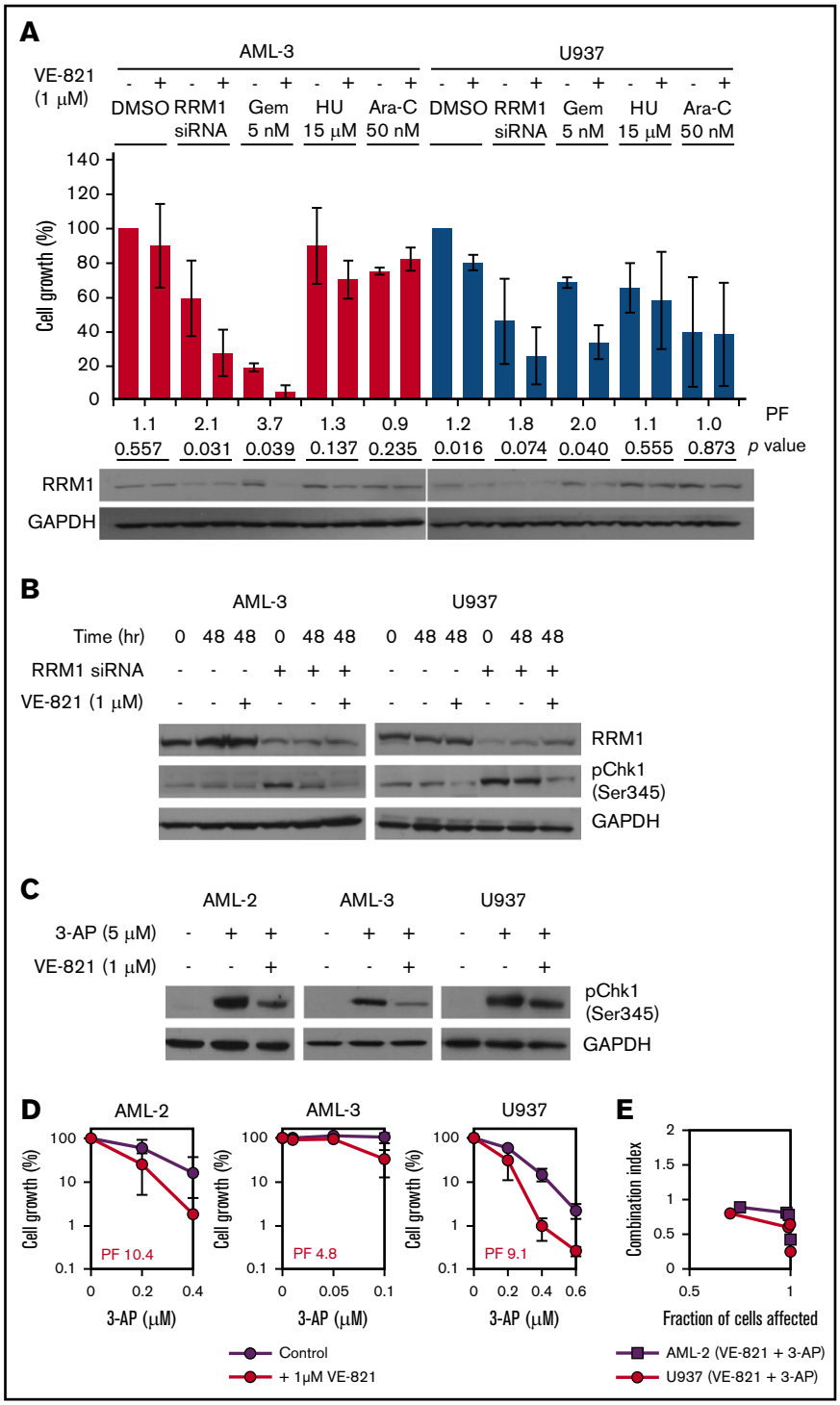

Figure 3. The cytotoxic effect of RNR inhibition via siRNA-mediated gene knockdown or 3-AP treatment is potentiated by VE-821. (A) AML-3 (red bars) and U937 cells (blue bars) were treated with RNR RRM1 siRNA (24 hours before dosing), 5 nM Gem, 15 μM HU, 50 nM Ara-C, or vehicle control in the presence of 1 μM VE-821 or DMSO control. Cell survival was determined after 48 hours, and the bar chart shows cell growth relative to vehicle controls. Numbers below bars represent the VE-821-induced potentiation factor (PF) and *P* values for each treatment determined by a 2-tailed Student *t* test. Western blotting for RRM1 was also performed 48 hours posttreatment (below the bar chart). (B) AML-3 (left) and U937 cells (right) with and without siRNA-mediated RRM1 knockdown were treated with 1 μM VE-821 (or DMSO control) for 48 hours, and western blotting was performed for RRM1 and pCHK1 (Ser345). (C) AML-2, AML-3, and U937 cells were treated with 5 μM 3-AP (or vehicle control) in the presence of 1 μM VE-821 (or DMSO control) for 2 hours, and western blotting was performed for pCHK1 (Ser345). (D) AML-2, AML-3, and U937 cells were treated with 3-AP alone (purple circles) or in combination with 1 μM VE-821 (red circles), and cell survival (relative to respective vehicle controls) was determined after 96 hours. PFs were calculated at the highest dose of 3-AP. For all western blots, GAPDH was used as a loading control, and for potentiation assays, data represent the mean ± SD of 3 independent experiments.

Discussion

Targeting components of the DDR is an attractive approach for treating cancers that harbor high levels of endogenous replication stress considering that many anticancer treatments function primarily in S phase via inhibition of DNA replication. However, the identification of efficacious drug combinations remains challenging given the extensive genetic heterogeneity intrinsic to most cancers, including AML.

Evidence suggests that some cancers, such as those with MYC activation or *ARID1A* mutation, have sufficiently high endogenous levels of replication stress to justify use of ATRi as monotherapy.[23-26] Despite evidence of synthetic lethality with activated oncoproteins in other cancer models, we observed only very modest single-agent ATRi activity in AML. Our data and data from the majority of published preclinical studies suggest a strategy in which ATR inhibitors are likely to be most efficacious in

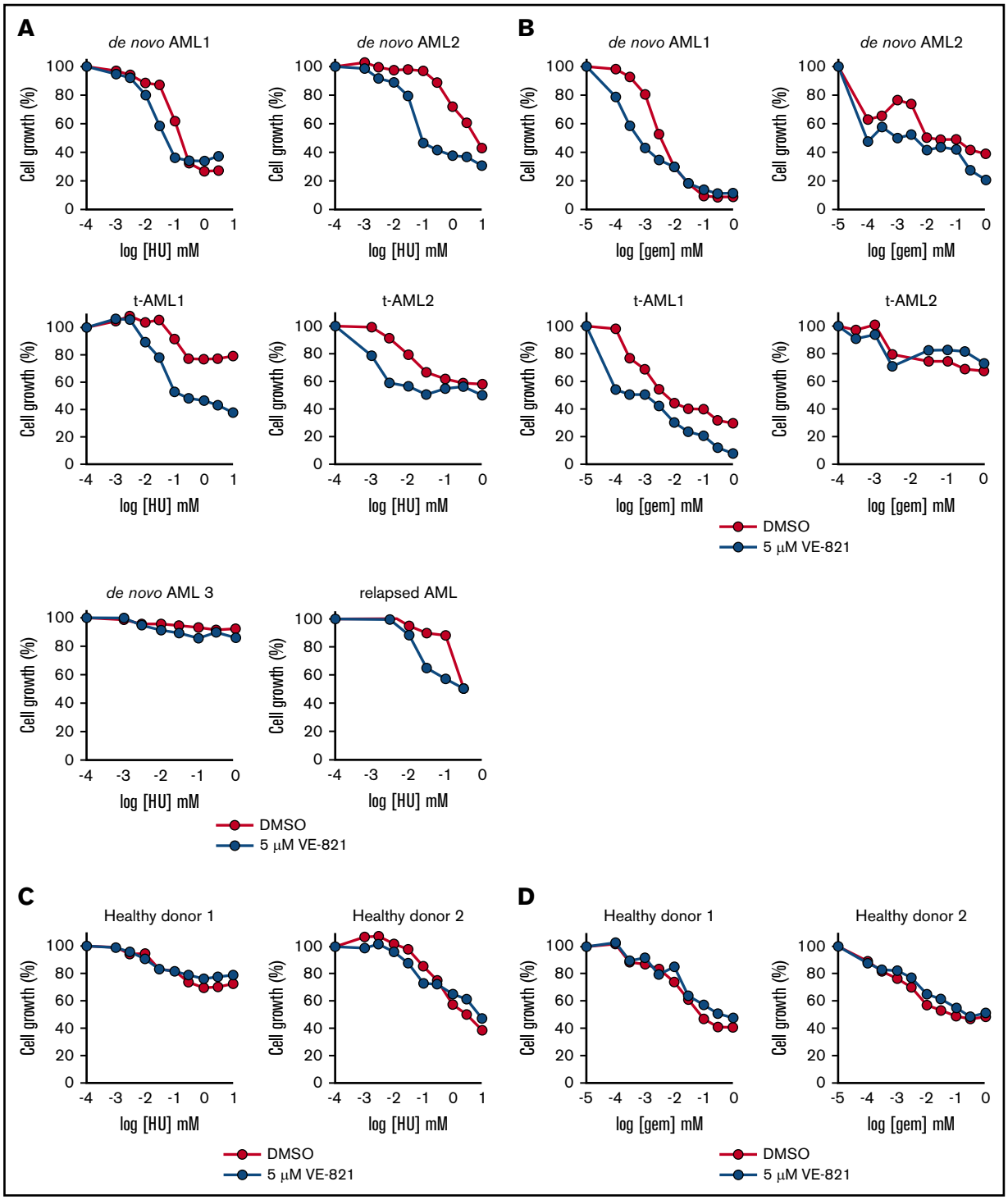

Figure 4. VE-821-mediated ATR inhibition potentiates the cytotoxic effects of HU and Gem in mononuclear cells isolated from AML patients. (A-B) Bone marrow mononuclear cells from up to 6 AML patients (3 de novo AML, 1 relapsed AML, and 2 t-AML patients) were treated with (A) HU or (B) Gem in combination with 5 μM VE-821 (blue circles) or DMSO control (red circles). Cell survival (relative to respective vehicle controls) was determined after 72 hours by addition of resazurin sodium salt. (C-D) $CD34^+$ cells from 2 healthy donors were treated with (C) HU or (D) Gem, and cell survival was determined as above. See supplemental Figure 5C.

combination with therapy that generates additional replication stress.[22,27,28] Specifically, we show here that ATR inhibition is particularly effective in combination with hydroxyurea and gemcitabine, agents that induce replication fork collapse, suggesting that overreliance on the DDR machinery renders AML cells particularly susceptible to ATR inhibition.

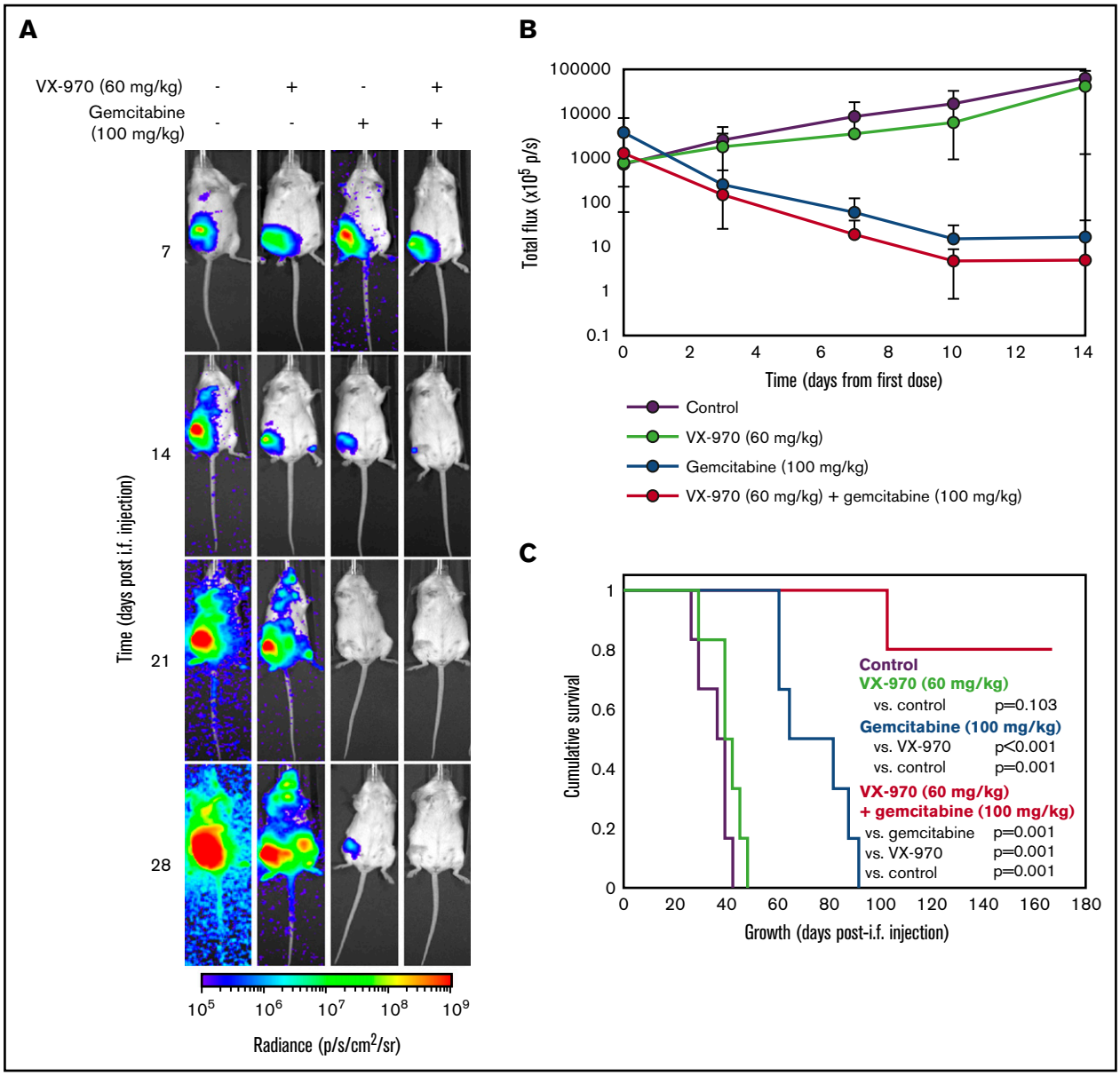

Figure 5. Cotreatment with Gem and VX-970 confers early disease control and increased overall survival in an orthotopic mouse model of AML. (A) Twenty-four female *Rag2*$^{-/-}$*gc*$^{-/-}$ mice were injected intrafemorally (i.f.) with 5 × 10^5 MV4-11 luc$^+$GFP$^+$ cells, and treatment with 60 mg/kg VX-970, 100 mg/kg Gem, or both (or vehicle controls) was administered 7 to 21 days after injection, as detailed in the main article text. Bioluminescent imaging was performed at regular intervals to monitor disease burden. Shown are representative mice from each treatment arm at 7, 14, 21, and 28 days after injection. (B) Total flux (used to quantify disease burden) was measured from bioluminescent images during the treatment period. Data represent the mean ± SD for 6 mice in each treatment arm on indicated days after administration of the first dose. Some of the lower error bars (SD) have been omitted because they cannot be plotted on a log scale. (C) Overall event-free survival in each treatment arm was compared by Kaplan-Meier survival analysis. At termination of study on day 165, 4 mice in the VX-970 and Gem cotreatment arm remained alive and disease-free. See supplemental Figure 6. p/s/cm^2/sr, photons per second per centimeter squared per steradian.

We show that loss of RNR induces a pCHK1 response and attenuates proliferation in AML cells that is potentiated by inhibition of ATR. These data suggest that stalled replication forks resulting from RNR inhibition are signaled via ATR and are highly repairable via downstream pathways. In this scenario, ATR functional status is a major determinant of AML cell fate, suggesting a mechanism to explain why the antileukemic activity of gemcitabine and hydroxyurea, both inhibitors of RNR, are significantly potentiated by ATRi. Of potential importance, inhibition of RNR by hydroxyurea is reversible, whereas inhibition by gemcitabine is irreversible.[29] Consistent with this, we observed a significantly longer induction of pCHK1 after single-agent gemcitabine treatment compared with hydroxyurea (data not shown).

The prevailing data suggest a mechanism whereby targeting ATR is particularly effective at inducing cell death in the setting of high

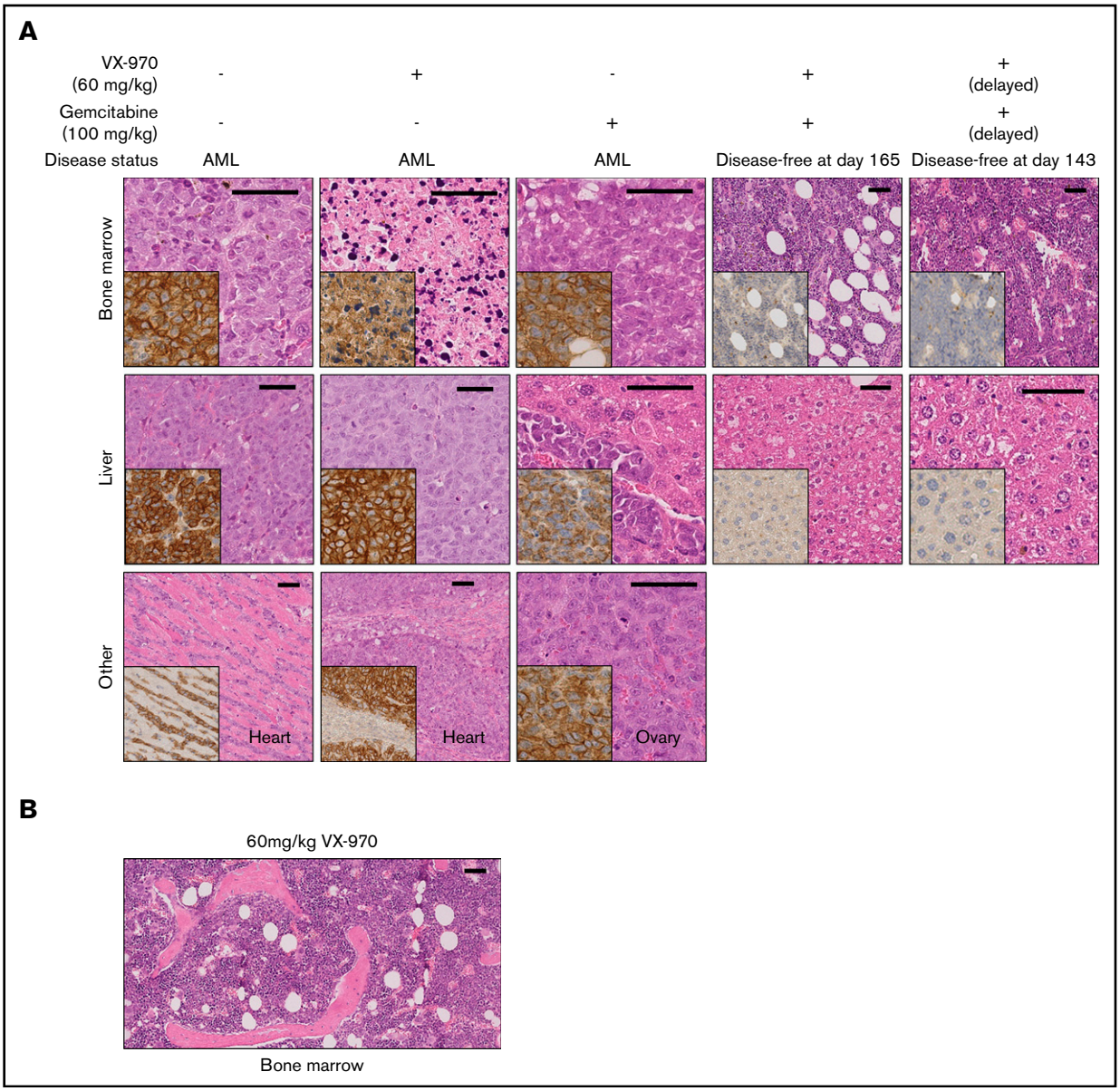

Figure 6. Postmortem immunohistochemical examination of mouse tissues confirms eradication of MV4-11 cells in mice cotreated with Gem and VX-970. (A) Bone marrow (from injected femur), liver, and other tumors (as indicated) were stained with hematoxylin and eosin (large images), human CD33 (insets), human CD45 (not shown), and human Ki67 (not shown). Images are from a representative mouse in each treatment arm (for vehicle treated, VX-970 monotherapy, and Gem monotherapy) using tissues taken at the point of death (specified humane end point) to confirm the presence of human AML cells. For the VX-970 and Gem cotreatment arm (including localized and disseminated [delayed treatment] AML), disease-free mice are shown, confirming normal morphology and eradication of leukemic cells. (B) Hematoxylin and eosin staining of bone marrow from a nonengrafted mouse after treatment with 60 mg/kg VX-970 for 5 consecutive days. Scale bars represent 10 μm.

and sustained levels of replication stress resulting from stalled replication. In support of this hypothesis, ATRi is effective when delivered in combination with small molecular inhibitors of both de novo (RNR) and salvage (deoxycytidine kinase) nucleotide biosynthesis pathways.[30] Inhibition of either of these pathways results in lower dNTP levels and induces stalled replication forks, but loss of 1 pathway can be partly compensated by upregulation of the other.[31] However, simultaneous inhibition of both pathways is particularly effective at inducing sustained replication stress, rendering cells susceptible to ATRi.[30] Our data demonstrate that this model can be therapeutically exploited via the use of ATR inhibitors in combination with hydroxyurea or gemcitabine, clinically approved agents that directly abrogate RNR function that compromise dNTP pools and induce replication stress.[17,18] Furthermore, evidence suggests that ATR signaling also plays a direct role in regulating dNTP metabolism. Inhibition of ATR reduces dNTP levels in cancer cell lines,[32] which has been linked to inhibition of the RNR RRM2 subunit.[6,33] Le and colleagues[30] demonstrated downregulation of both RRM1 and RRM2 in lymphoblastic leukemia cells after ATR inhibition, and targeted knockdown of RRM2 attenuates the deoxycytidine monophosphate pool and reduces incorporation of deoxycytidine triphosphate into replicating DNA.[30] These data demonstrate that

ATR inhibitors gemcitabine and hydroxyurea can have an effect on dNTP pools via inhibition of RNR.

Analogs of fludarabine and cladribine also have some RNR inhibitory activity, although it is reversible,[34,35] which might explain potentiation by ATRi in some AML cell lines. However, analogs of cytarabine do not inhibit RNR,[36] and although we observed cytarabine-induced pCHK1 in some AML cell lines that was attenuated by ATRi (data not shown), there was no consistent evidence that ATR inhibition or knockdown potentiated cytarabine-induced growth inhibition, cell cycle progression, or replication fork progression. However, ATRi inhibition did potentiate the growth inhibitory effects of cytarabine in THP-1 AML cells, consistent with data reported by others.[37] It remains possible that somatic genetic background could affect sensitivity to ATR inhibitors in combination with cytarabine. It is also possible that higher doses of ATR inhibitor might potentiate cytarabine-induced growth inhibition. The prevailing evidence suggests that cytarabine-induced stalled replication forks are repaired inefficiently via ATR-mediated mechanisms compared with those arising as a result of RNR inhibition and also that the contribution made by ATR to repair may be modified by somatic genetic background.

Our data warrant clinical investigation of ATR inhibitors as AML therapy in combination with agents that target RNR, including gemcitabine and hydroxyurea. In addition to demonstrated efficacy and widespread clinical use for solid malignancies, gemcitabine has clinical activity with acceptable toxicity in refractory and relapsed AML.[38-41] Data from a phase 1 trial of gemcitabine in solid tumors provides evidence of its activity in combination with VX-970.[42] Hydroxyurea also has efficacy in AML and is primarily used in a palliative setting for leukocytoreduction, particularly in elderly patients with low tolerance for more aggressive therapies.[43] Gemcitabine inhibits the RRM1 subunit, whereas hydroxyurea inhibits the catalytic RRM2 subunit.[44] We show that depletion of RRM1 or inhibition of RRM2 both synergize with ATR inhibition, demonstrating that potentiation by ATRi is not RNR subunit specific. We observed potentiation of 3-AP–induced growth inhibition by VE-821, suggesting that direct targeting of RNR in combination with ATRi could prove efficacious in the treatment of AML. Early phase clinical trials of 3-AP demonstrate efficacy in aggressive myeloproliferative neoplasms and refractory AML with an acceptable safety profile,[45-50] which paves the way toward proof-of-concept studies in combination with ATR inhibitors.

In summary, our data demonstrate that administration of an ATR inhibitor at biologically effective doses is well tolerated in a murine model, with no apparent effects on normal marrow morphology. Furthermore, we show that ATRi significantly potentiates the activity of hydroxyurea and gemcitabine in AML cells. ATR loss is synergistic with inhibition of RNR, which identifies this as a mechanism that potentially explains the potency of combinations incorporating ATRi and agents that target RNR. The generation of a therapeutic window via administration of an intrinsically nontoxic ATR inhibitor could be particularly important for elderly AML patients who often have low tolerance for standard remission induction regimens. Our findings will also inform the deployment of ATR inhibitors for the treatment of AML and other hematologic malignancies.

Acknowledgments

This work was supported by a specialist program grant from Bloodwise (13044) (J.M.A.), by the JGW Patterson Foundation (J.M.A.), by the Medical Research Council/Engineering and Physical Sciences Research Council Newcastle Molecular Pathology Node, and by a National Centre for the Replacement, Retirement, and Reduction of Animals in Research fellowship (D.P.). The IVIS Spectrum In Vivo Imaging System was funded by Wellcome Trust grant 087961.

No funding or reagents were received from Vertex Pharmaceuticals in support of the project described in this article.

Authorship

Contribution: S.E.F. helped conceive the study, design the experiment, generate and analyze data, and write the manuscript; H.J.B. and C.J.E. helped design the experiment and generate and analyze data; R.P., Y.D., N.J.C., O.H., D.P., D.J., C.P., P.M., G.H.J., H.J.M., T.M., and G.L.J. provided key reagents and helped interpret data; J.P. and S.F. advised on the use of small molecule inhibitors and data interpretation; and J.M.A. directed the research, conceived the study, secured funding, designed the experiment, analyzed data, and wrote the manuscript with editorial assistance from all other authors.

Conflict-of-interest disclosure: J.P. is an employee of Vertex Pharmaceuticals. S.F. is a former Vertex employee and holds stock ownership in Vertex. N.J.C. has received research funding from Vertex Pharmaceuticals for a Medical Research Council (MRC) industrial Collaborative Awards in Science and Engineering (CASE) studentship on ATR (1 October 2010 to 30 September 2014) and currently has research funding from Merck for an MRC industrial CASE studentship on ATR (1 October 2016 to 30 September 2020). The remaining authors declare no competing financial interests.

Correspondence: James M. Allan, Newcastle Cancer Centre, Northern Institute for Cancer Research, Paul O'Gorman Building, Newcastle University, Newcastle upon Tyne NE2 4HH, United Kingdom; e-mail: james.allan@newcastle.ac.uk.

References

1. Gaillard H, García-Muse T, Aguilera A. Replication stress and cancer. *Nat Rev Cancer*. 2015;15(5):276-289.
2. Zou L, Elledge SJ. Sensing DNA damage through ATRIP recognition of RPA-ssDNA complexes. *Science*. 2003;300(5625):1542-1548.
3. Jazayeri A, Falck J, Lukas C, et al. ATM- and cell cycle-dependent regulation of ATR in response to DNA double-strand breaks. *Nat Cell Biol*. 2006;8(1):37-45.
4. Toledo LI, Altmeyer M, Rask MB, et al. ATR prohibits replication catastrophe by preventing global exhaustion of RPA. *Cell*. 2013;155(5):1088-1103.
5. Couch FB, Bansbach CE, Driscoll R, et al. ATR phosphorylates SMARCAL1 to prevent replication fork collapse. *Genes Dev*. 2013;27(14):1610-1623.
6. Buisson R, Boisvert JL, Benes CH, Zou L. Distinct but concerted roles of ATR, DNA-PK, and Chk1 in countering replication stress during S phase. *Mol Cell*. 2015;59(6):1011-1024.

7. Roman E, Smith A, Appleton S, et al. Myeloid malignancies in the real-world: occurrence, progression and survival in the UK's population-based Haematological Malignancy Research Network 2004-15. *Cancer Epidemiol*. 2016;42:186-198.

8. Halazonetis TD, Gorgoulis VG, Bartek J. An oncogene-induced DNA damage model for cancer development. *Science*. 2008;319(5868):1352-1355.

9. Maya-Mendoza A, Ostrakova J, Kosar M, et al. Myc and Ras oncogenes engage different energy metabolism programs and evoke distinct patterns of oxidative and DNA replication stress. *Mol Oncol*. 2015;9(3):601-616.

10. Dobbelstein M, Sørensen CS. Exploiting replicative stress to treat cancer. *Nat Rev Drug Discov*. 2015;14(6):405-423.

11. Traggiai E, Chicha L, Mazzucchelli L, et al. Development of a human adaptive immune system in cord blood cell-transplanted mice. *Science*. 2004; 304(5667):104-107.

12. Chou TC, Talalay P. Quantitative analysis of dose-effect relationships: the combined effects of multiple drugs or enzyme inhibitors. *Adv Enzyme Regul*. 1984;22:27-55.

13. Groth P, Ausländer S, Majumder MM, et al. Methylated DNA causes a physical block to replication forks independently of damage signalling, O(6)-methylguanine or DNA single-strand breaks and results in DNA damage. *J Mol Biol*. 2010;402(1):70-82.

14. Peasland A, Wang LZ, Rowling E, et al. Identification and evaluation of a potent novel ATR inhibitor, NU6027, in breast and ovarian cancer cell lines. *Br J Cancer*. 2011;105(3):372-381.

15. Zeman MK, Cimprich KA. Causes and consequences of replication stress. *Nat Cell Biol*. 2014;16(1):2-9.

16. Aye Y, Li M, Long MJ, Weiss RS. Ribonucleotide reductase and cancer: biological mechanisms and targeted therapies. *Oncogene*. 2015;34(16): 2011-2021.

17. Singh A, Xu YJ. The cell killing mechanisms of hydroxyurea. *Genes (Basel)*. 2016;7(11).

18. Guo JR, Chen QQ, Lam CW, et al. Profiling ribonucleotide and deoxyribonucleotide pools perturbed by gemcitabine in human non-small cell lung cancer cells. *Sci Rep*. 2016;6(1):37250.

19. Weber AM, Ryan AJ. ATM and ATR as therapeutic targets in cancer. *Pharmacol Ther*. 2015;149:124-138.

20. Kolberg M, Strand KR, Graff P, Andersson KK. Structure, function, and mechanism of ribonucleotide reductases. *Biochim Biophys Acta*. 2004; 1699(1-2):1-34.

21. Liu S, Ge Y, Wang T, et al. Inhibition of ATR potentiates the cytotoxic effect of gemcitabine on pancreatic cancer cells through enhancement of DNA damage and abrogation of ribonucleotide reductase induction by gemcitabine. *Oncol Rep*. 2017;37(6):3377-3386.

22. Fokas E, Prevo R, Pollard JR, et al. Targeting ATR in vivo using the novel inhibitor VE-822 results in selective sensitization of pancreatic tumors to radiation. *Cell Death Dis*. 2012;3(12):e441.

23. Murga M, Campaner S, Lopez-Contreras AJ, et al. Exploiting oncogene-induced replicative stress for the selective killing of Myc-driven tumors. *Nat Struct Mol Biol*. 2011;18(12):1331-1335.

24. Höglund A, Nilsson LM, Muralidharan SV, et al. Therapeutic implications for the induced levels of Chk1 in Myc-expressing cancer cells. *Clin Cancer Res*. 2011;17(22):7067-7079.

25. Williamson CT, Miller R, Pemberton HN, et al. ATR inhibitors as a synthetic lethal therapy for tumours deficient in ARID1A. *Nat Commun*. 2016;7:13837.

26. Morgado-Palacin I, Day A, Murga M, et al. Targeting the kinase activities of ATR and ATM exhibits antitumoral activity in mouse models of MLL-rearranged AML. *Sci Signal*. 2016;9(445):ra91.

27. Jossé R, Martin SE, Guha R, et al. ATR inhibitors VE-821 and VX-970 sensitize cancer cells to topoisomerase i inhibitors by disabling DNA replication initiation and fork elongation responses. *Cancer Res*. 2014;74(23):6968-6979.

28. Prevo R, Fokas E, Reaper PM, et al. The novel ATR inhibitor VE-821 increases sensitivity of pancreatic cancer cells to radiation and chemotherapy. *Cancer Biol Ther*. 2012;13(11):1072-1081.

29. Heinemann V, Xu YZ, Chubb S, et al. Inhibition of ribonucleotide reduction in CCRF-CEM cells by 2′,2′-difluorodeoxycytidine. *Mol Pharmacol*. 1990; 38(4):567-572.

30. Le TM, Poddar S, Capri JR, et al. ATR inhibition facilitates targeting of leukemia dependence on convergent nucleotide biosynthetic pathways. *Nat Commun*. 2017;8(1):241.

31. Nathanson DA, Armijo AL, Tom M, et al. Co-targeting of convergent nucleotide biosynthetic pathways for leukemia eradication. *J Exp Med*. 2014; 211(3):473-486.

32. Pfister SX, Markkanen E, Jiang Y, et al. Inhibiting wee1 selectively kills histone H3K36me3-deficient cancers by dNTP starvation. *Cancer Cell*. 2015; 28(5):557-568.

33. Bester AC, Roniger M, Oren YS, et al. Nucleotide deficiency promotes genomic instability in early stages of cancer development. *Cell*. 2011; 145(3):435-446.

34. Aye Y, Stubbe J. Clofarabine 5′-di and -triphosphates inhibit human ribonucleotide reductase by altering the quaternary structure of its large subunit. *Proc Natl Acad Sci USA*. 2011;108(24):9815-9820.

35. Tseng WC, Derse D, Cheng YC, Brockman RW, Bennett LL Jr. In vitro biological activity of 9-beta-D-arabinofuranosyl-2-fluoroadenine and the biochemical actions of its triphosphate on DNA polymerases and ribonucleotide reductase from HeLa cells. *Mol Pharmacol*. 1982;21(2):474-477.

36. Moore EC, Cohen SS. Effects of arabinonucleotides on ribonucleotide reduction by an enzyme system from rat tumor. *J Biol Chem*. 1967;242(9): 2116-2118.

37. Ma J, Li X, Su Y, et al. Mechanisms responsible for the synergistic antileukemic interactions between ATR inhibition and cytarabine in acute myeloid leukemia cells. *Sci Rep*. 2017;7:41950.

38. Gandhi V, Plunkett W, Du M, Ayres M, Estey EH. Prolonged infusion of gemcitabine: clinical and pharmacodynamic studies during a phase I trial in relapsed acute myelogenous leukemia. *J Clin Oncol*. 2002;20(3):665-673.

39. Advani AS, Shadman M, Ali-Osman F, et al. A phase II trial of gemcitabine and mitoxantrone for patients with acute myeloid leukemia in first relapse. *Clin Lymphoma Myeloma Leuk*. 2010;10(6):473-476.

40. Kolb EA, Steinherz PG. A new multidrug reinduction protocol with topotecan, vinorelbine, thiotepa, dexamethasone, and gemcitabine for relapsed or refractory acute leukemia. *Leukemia*. 2003;17(10):1967-1972.

41. Rizzieri DA, Ibom VK, Moore JO, et al. Phase I evaluation of prolonged-infusion gemcitabine with fludarabine for relapsed or refractory acute myelogenous leukemia. *Clin Cancer Res*. 2003;9(2):663-668.

42. Plummer ER, Dean EJ, Evans TRJ, et al. Phase I trial of first-in-class ATR inhibitor VX-970 in combination with gemcitabine (Gem) in advanced solid tumors (NCT02157792) [abstract]. *J Clin Oncol*. 2016;34. Abstract 2513.

43. Ossenkoppele G, Löwenberg B. How I treat the older patient with acute myeloid leukemia. *Blood*. 2015;125(5):767-774.

44. Wright JA, Chan AK, Choy BK, Hurta RA, McClarty GA, Tagger AY. Regulation and drug resistance mechanisms of mammalian ribonucleotide reductase, and the significance to DNA synthesis. *Biochem Cell Biol*. 1990;68(12):1364-1371.

45. Gojo I, Tidwell ML, Greer J, et al. Phase I and pharmacokinetic study of triapine, a potent ribonucleotide reductase inhibitor, in adults with advanced hematologic malignancies. *Leuk Res*. 2007;31(9):1165-1173.

46. Giles FJ, Fracasso PM, Kantarjian HM, et al. Phase I and pharmacodynamic study of triapine, a novel ribonucleotide reductase inhibitor, in patients with advanced leukemia. *Leuk Res*. 2003;27(12):1077-1083.

47. Odenike OM, Larson RA, Gajria D, et al. Phase I study of the ribonucleotide reductase inhibitor 3-aminopyridine-2-carboxaldehyde-thiosemicarbazone (3-AP) in combination with high dose cytarabine in patients with advanced myeloid leukemia. *Invest New Drugs*. 2008;26(3):233-239.

48. Yee KW, Cortes J, Ferrajoli A, et al. Triapine and cytarabine is an active combination in patients with acute leukemia or myelodysplastic syndrome. *Leuk Res*. 2006;30(7):813-822.

49. Karp JE, Giles FJ, Gojo I, et al. A phase I study of the novel ribonucleotide reductase inhibitor 3-aminopyridine-2-carboxaldehyde thiosemicarbazone (3-AP, Triapine) in combination with the nucleoside analog fludarabine for patients with refractory acute leukemias and aggressive myeloproliferative disorders. *Leuk Res*. 2008;32(1):71-77.

50. Zeidner JF, Karp JE, Blackford AL, et al. A phase II trial of sequential ribonucleotide reductase inhibition in aggressive myeloproliferative neoplasms. *Haematologica*. 2014;99(4):672-678.